Crustal deformation studies in the northern part of Aswan Lake using GPS technique

Hamed, M.* ; Abdel- Monem S. M.; Mahmoud, S. **; Shaker, A.***; Saad, A.*****

***** *Faculty of Engineering, Kafer Elshekh University.*

****** *National Recearch Institute of Astronomy and Geophysic*

******* *Shoubra faculty of Engineering, Banha University.*

Abstract

Study of recent crustal movements is considered as an important task for geodesists, geologists and geophysicists. This is due to other part this phenomena is very dangerous on the human life in the world, so all constructed projects must be secured against the crustal deformation at local, regional and global scales. Study of recent crustal movements means the determination of the magnitude, direction and the rate of these movements. In addition, the analysis of horizontal crustal strains is important in a wide area of geophysical studies as well as in earthquake prediction. Nowadays, crustal deformation within Egypt relates to the regional and local tectonic forces. GPS data were collected and processed using Bernese 5.0 software. The displacement vectors for each epoch of observation were calculated from the coordinate changes. Considering the confidence limit, most of these displacement vectors could be mainly attributed to the movement within Aswan study area in those epochs of measurements. The relative movements between the epochs of measurements are estimated. The main objective of this work is to monitor the surface crustal deformation around the reservoir for understanding the geodynamics of this region. Also, an attempt has been made to investigate the recent crustal movements by two solutions , by making the point in the network once as a fixed point and once again by connecting point (IGS) out of the network and their relation to the induce seismicity in the areas vicinity of Aswan Lake

Keywords: Aswan region, GPS observations, deformation parameters calculation and interpretation.

Introduction

The use of geodetic techniques to study the movement of the Earth's surface is based upon repeated measurements of geodetic stations fixed on the Earth's surface. The position of these stations can be determined using terrestrial or space techniques (GPS). It must be known

that, the results of repeated measurements to determine the position of the same point is the main source of information on recent movement of the Earth's surface. In order to get useful information, the proper time interval between two repeated measurements must be carefully determined to suite the deformation state (**Vyskočil 1989**). Monitoring recent crustal movements has become one of the major and important tasks facing geodesists, since it has vital consequences for human safety and economic achievements. There are a variety of geodetic and other techniques that are currently in use for monitoring such deformations on all local, regional and global scales. In fact, the recent crustal movements nowadays have several implications in the Egyptian territory.

Aswan region is located within the stable platform of Arabio-Nubian Massif. The Nile follows the contact between surface exposure of the granite of the Eastern Desert to the East, and the sedimentary cover of the Nubian sandstone to the West. The Nubian plain covers most of the area southwest of Aswan city and borders of the reservoir from the West **(Issawi, 1969; 1978)**. The Nubian plain is relatively flat, and the surface has an average elevation of 200 m above the mean Sea-level and has very little relief. The Nubian Plain is interrupted by sandstone hills composed of resistant beds of the Nubian Formation as well as limestone hills as Gebel Marawa (274 m). The structural pattern of Aswan region is governed mainly by faulting. The faults crossing the region are classified into E-W and N-S faults (Fig. 1). The N-S faults are well represented in the vicinity of the reservoir and affect the sandstone beds of the Nubian plain.

Aswan region nowadays is one of the most important regions from the tectonic of view. It is not difficult to visualize that the High Dam is affecting the whole country, since it provides Egypt with water needed for human activities and with electricity that is needed for industry and development **(Abdel-Monem, 2001)**. Consequently, the safety of the Dam and its surrounding vicinity is of ultimate concern to all Egyptian respective communities. For this reason, a seismic network was installed to monitor the earthquake activity continuously within Aswan region. The seismicity recorded by Aswan Seismic Network is located at the intersection between the E-W and N-S fault trends **(Abdel-Monem, 2005)**. The magnitudes of these earthquakes are ranging from 0.1 to 4.8 occurred over the entire Aswan region during the period from 1982 to 2009 as shown as in figure (1) **(Abdel-Monem, 2010)**.

Several systems of local and sub-regional geodetic networks have been established around active faults, in order to monitor crustal deformation associated with the earthquake activity and to understand the geodynamics of the area. This paper focuses on the present state of crustal

deformation studies at Aswan region using the precise geodetic measurements and by two solutions.

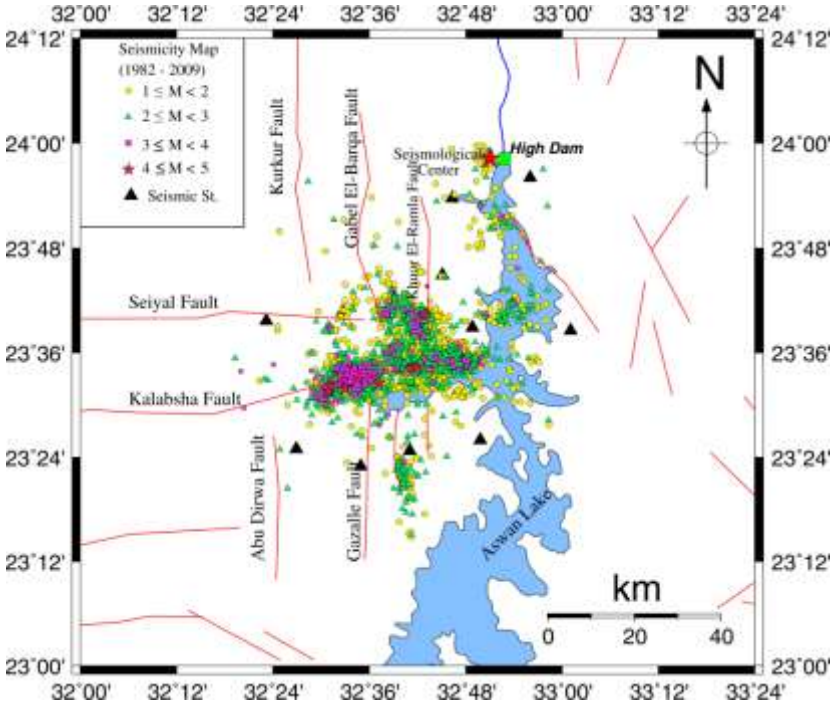

Fig. 1: Micro-earthquakes recorded by Aswan seismic network from 1982 to 2009 .
——— Faults taken from map by Issawi,(1969).

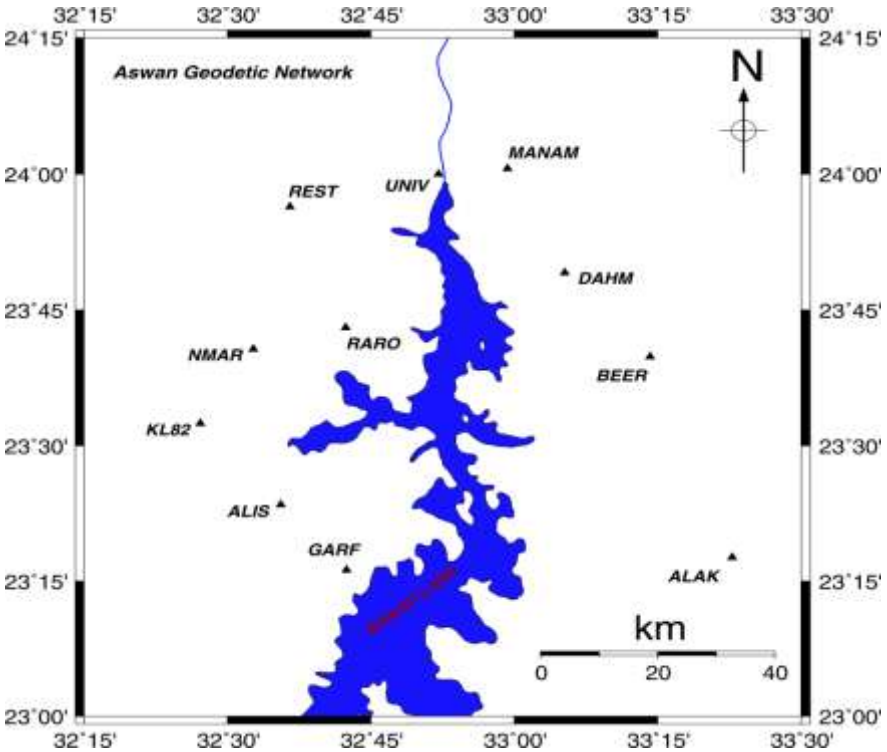

Figure (1): Configuration of the regional geodetic network.

Table (1): Names of stations, their codes (ID) and files abbreviations

Station Name	Codes (ID)	Files Abbreviations
Wadi Al-Alaki	ALAK	AL
Beer Om Hebal	BEER	BE
Dahmeet	DAHM	DA
Kalabsha 82	KL 82	KL
Manam	MNAM	MA
North Marawa	NMAR	NM
Rawraw	RARO	RA
University	UNIV	UN
Rest	REST	RS
Gabel Alisa	ALIS	AS
Garf Hussein	GARF	GA

GPS measurements and data analysis

GPS technique has become the geodetic method of choice for studying a wide range of geophysical phenomena. GPS measurements are now in use to determine the motion of the Earth's tectonic plates, and to study deformation around active faults. It has been known for a long time already that reservoir-induced deformation result from accumulation of large mass of water **(Rothe, 1968; Sohrab, 1972)**. To monitor such a deformation, arrays of points surrounding particular dams and neighboring area are established. The geodetic observations were carried out by terrestrial technique (1983 – 1995). The terrestrial technique had been replaced by the GPS technique since 1997. The data were collected from Aswan geodetic network, which consists of 11 stations and is covering the northern part of Aswan Lake. There are 7 stations along western side of Lake Aswan and 4 stations along the eastern side of the Lake as shown in figure (2). Table (1) shows the names of stations, their codes (ID) and files abbreviations. The campaign observations are repeated twice a year since 1997 till now. GPS surveys had been carried out by researchers from National Research Institute of Astronomy and Geophysics (NRIAG) . The GPS observations are carried out using Trimble receivers 4000SSE and SSI under constant conditions, such as: the satellite-masking angle is of 15 degrees, the sampling interval is 30 seconds and

observation time in all sessions is 72 hours at all stations. The available GPS data (2006 – 2010) were used in the present work. GPS data were processed using Bernese software version 5.0 (developed by the University of Bern Brockmann, 1996).

Generally, geodetic monitoring networks are divided into relative and reference networks **(Caspary, 1987)**. In the first case, the network is divided into two sub-nets, by a geological feature. In this case, only relative displacements between the blocks of object points can be determined. In the second case, the network consists of a reference and an object part. The reference station could be internal or external station of the network. The determination of displacements of the object points relative to the reference is the goal of the analysis. A confirmation of the stability of reference points is the only aim of the measurements in the reference network. The annual rates of the displacement vectors at each GPS station in our case are obtained under two methods of solution.

In the test area (Aswan Regional Network), data of five GPS campaigns of (Nov. 2006 to Jun. 2007), (Jun. 2007 to Jan. 2008), (Jan.2008 to Jun.2009), (Jun. 2009 to March.2010) and (Nov. 2006 to March.2010) as shown as in table (2) were processed, using the Bernese software version 5.0 (**Dach, 2007)**. The pervious two solutions were used in the processing and adjustment, in our case, in order to know which method can be used in the future.

Table (2): Campaign information

Item	**Campaign**				
	Campaign No.1	**Campaign No.2**	**Campaign No.3**	**Campaign No.4**	**Campaign No.5**
No. of sessions /day	1	1	1	1	1
Observation Period	24 h	24 h	24h	24 h	24h
Julian date	332	157	357	005	85
GPS week	1403	1430	1511	1460	1756
Interval	30sec	30sec	30sec	30sec	30sec
Masking angle	15^0	15^0	15^0	15^0	15^0

The first method : the network was processed and adjusted using the National reference station (RARO) as a fixed station (internal station), where it lies in the middle of the network .This method represent small and medium baselines length so the tropospheric model fitting is Saastamonen.

The second method :

In this way, we have taken an IGS station as outside station of the network (external station) namely (Drag, Israel) and it used as a fixed station or a reference station. This station is related to ITRF 2000. Taking into account these parts during the analysis:-

- Take only the baselines connecting the network stations of origin and reference point so that, these lengths are long base lines.
- Tropospheric model and therefore the appropriate in accordance with a previous study is Hopfield model (Magda H,2010) also take the impact of tides on the grid points.
- A comparative study is done between two methods to examine the advantages and disadvantage of each method.

The normal equations for all sessions of each campaign were stored. Then, these normal equations were combined to obtain final solutions for each campaign. Repeatability of station coordinates of the different campaigns was calculated to estimate the precision of coordinates; hence, the crustal deformation rates were estimated. Tables (3) , figure (3) and Table (4) represent the total displacement between epochs 2006 to 2010 and the deformation difference between base lines in two cases respectively .

Horizontal movement investigation

The components of the horizontal movements at each station of GPS network were computed from the differences of adjusted coordinates of the stations from one epoch to another and from the last epoch to the second. The velocity, error ellipses and the approximation of the field of horizontal displacements are determined for all geodetic points. The displacement vectors of each epoch of the observations were calculated according to the coordinate changes. Considering the confidence limit, most of these displacement vectors can be mainly attributed to the movement within the study area in those campaigns of measurements. The following analysis through all stages as shown as:

a- Period 2006-2007 when linking with (Drag)

The result of analysis through this period gives a small movement in most of the points such as (ALAK, BEER, DAHM, REST, UNIV). Moreover, it is identical to the situation of the region in this period compared to that when linking to (RARO) where gives a larger movement were found in the previous points. In addition, the previous points when linking to (Drag) give more reflective situation in the region surrounding these points.

b- Period 2007-2008 when linking with (Drag)

We find that the change in the movement appears to be logically compared to when linking with (RARO). For example, during the period 2006-2007, the point (ALAK) was moving from 0.8mm to -0.34mm in X-direction, from 1.15mm to -1.35mm in Y-direction and from 0.42mm to -0.21mm in Z-direction. This would be logically changed, and this includes most of the remaining points. However, in the case of the linking with (RARO), the movement is very large and the change seems to be not logically. Therefore, the change in X-direction was 4.0mm to 0.17mm, from 1.16mm to -2.51mm in Y-direction and from 0.4 mm to 1.19mm in Z-direction.

c- Period 2008-2009 when linking with (Drag)

Results converge at some points during this period and differ in the other. For example, the movement seems to be small at the point (ALAK) in this period compared to when linking with RARO.

d- Period 2009-2010 when linking with (Drag)

The movement is increasing when linking with (Drag) than in linking with (RARO), but this increasing of the movement seems to be small.

e- Period 2006 - 2010 when linking with (Drag)

Results converge at some stations during this period and differ in the other, but the direction of the displacement vectors on the most stations is approximately the same. For example, the movement seems to be the same at the points (ALAK, BEER and DAHM) and differ in the other points in this period compared to when linking with RARO. The movements and the mean square errors are accurate and appear to be logically compared to when linking with (RARO). This means that, linking the network with outside station gives more accurate results than if it is linked with inside station. Bernese software program gives more accurate results with long base lines than short base lines.

In this paper had been used the final analyses between the last epoch to the first one. The total rates of the horizontal displacement at each GPS station with 95% confidence error ellipses

ware determined (Table, 3 and Fig. 3). The error ellipses represent here the standard error in all direction around the observed site.

The horizontal displacement vectors in two cases are of small magnitude at the stations in the eastern part of the network. While the horizontal displacement vectors are large magnitude at the stations in the western part. Some stations of the network indicate significant changes while other stations illustrate negligible changes through the period of observations (Fig. 3).

Table (3): The total displacements between epochs 2006-2010 (using RARO as reference)

Station	Horizontal displacement and RMS in mm during the periods between from 2006 to 2010									
			RARO Reference				Drag Reference			
	Longitude	Latitude	dλ	RMS (dλ)	dφ	RMS (dφ)	dλ	RMS (dλ)	dφ	RMS (dφ)
DRAG	35 23 31.456392	31 35 35.522928	-	-	-	-	**-0.2**	**1.1**	**0.8**	**1.1**
RARO	32 42 21.715392	23 43 7.851114	**0.0**	**0.9**	**0.00**	**0.9**	-1.4	1.3	8.3	1.5
ALAK	33 22 49.271195	23 17 39.275167	1.7	1.2	-6.2	1.1	-0.7	1.2	3.8	1.5
BEER	33 14 13.503816	23 39 51.828556	-3.0	1.1	-6.1	1.0	-6.8	1.3	4.0	1.5
DAHM	33 5 17.106733	23 49 7.383057	1.0	1.1	-1.4	1.0	-3.6	1.3	5.4	1.5
GARF	32 42 28.447048	23 16 13.972213	3.3	1.0	-16.2	1.1	0.2	1.3	-6.8	1.5
ALIS	32 35 35.920502	23 23 26.281156	2.0	1.0	-2.75	1.1	-2.0	1.3	-18.2	1.5
MNAM	32 59 18.126748	24 0 54.441290	11.9	1.1	-13.9	1.1	9.3	1.5	-5.6	1.6
KL82	32 27 10.318852	23 32 27.428428	11.1	1.0	-9.3	1.0	7.9	1.3	1.0	1.5
NMRA	32 32 40.342816	23 40 40.875805	16.2	1.0	-13.1	1.0	12.5	1.3	-4.1	1.5
REST	32 36 33.650114	23 56 51.162487	7.8	1.0	-19.2	1.0	4.4	1.3	-10.9	1.5
UNIV	32 52 6.674907	24 0 7.022577	7.3	1.1	-13.6	1.1	6.1	1.6	-5.4	1.6

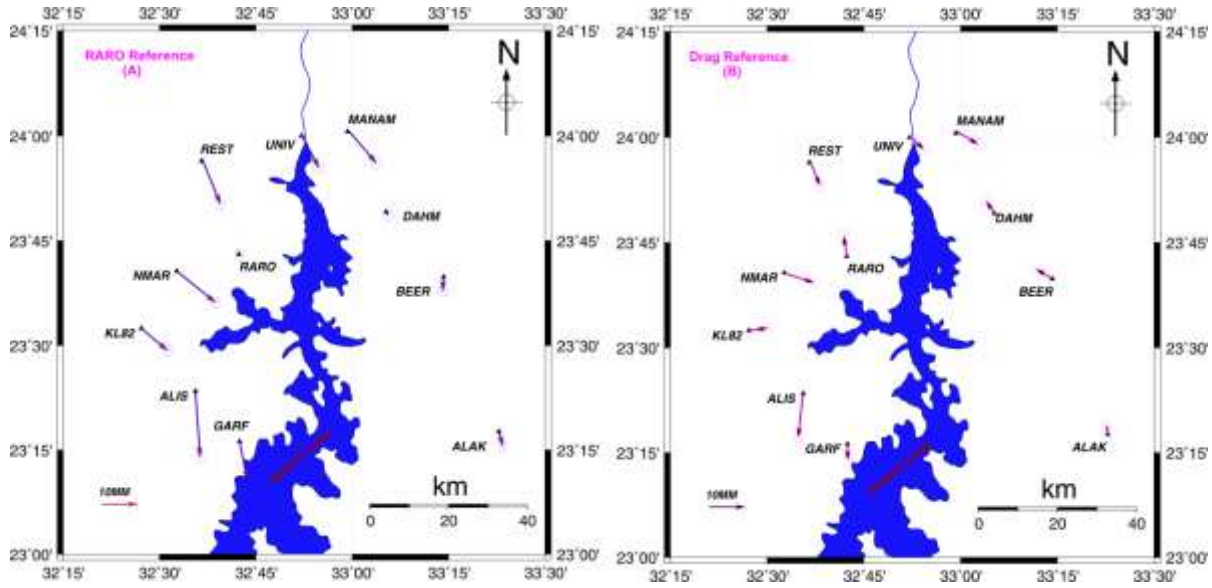

Figure (3): Total horizontal movements between the periods from 2006 to 2010 (using RARO and Drag as references)

Base lines Name	Base line from RARO2006	Base line from RARO2010	Diff1	Base line from DRAG 2006	Base line from DRAG 2006	Diff 2	Diff1-Diff2
ALAK-ALIS	811.929.410	811.929.334	0.0076	811.929.415	811.929.417	0.0002	0.0074
ALAK-GARF	688.504.682	688.504.636	٠,٠٠٤٦	688.504.685	688.504.688	٠,٠٠٠٣	0.0049
ALAK-BEER	435.315.625	435.315.619	٠,٠٠٠٦	435.315.632	435.315.627	٠,٠٠٠٥	0.0001
BEER-MANA	463.804.783	463.804.608	٠,٠١٧٥	463.804.800	463.804.634	٠,٠١٦٦	0.0009
MNAM-REST	392.924.379	392.924.420	٠,٠٠٤١-	392.924.372	392.924.453	٠,٠٠٨١-	0.004
REST-KL82	477.759.770	477.759.633	٠,٠١٣٧	477.759.786	477.759.664	٠,٠١٢٢	0.0015
RARO-DAHM	404.855.638	404.855.615	٠,٠٠٢٣	404.855.643	404.855.681	٠,٠٠٣٨-	0.0015
ALIS- NMRA	322.169.502	322.169.622	٠,٠١٢٠-	322.169.501	322.169.563	٠,٠٠٦٢-	-0.0058
MANM-NMRA	586.383.854	586.383.782	٠,٠٠٧٢	586.383.863	586.383.844	٠,٠٠١٩	0.0053
GARF-REST	756.532.071	756.532.006	٠,٠٠٦٥	756.532.089	756.532.032	٠,٠٠٥٧	0.0008
ALAK-REST	1.068.945.744	1.068.945.564	٠,٠١٨٠	1.068.945.758	1.068.945.602	٠,٠١٥٦	0.0024
BEER-REST	712.448.680	712.448.515	٠,٠١٦٥	712.448.691	712.448.552	٠,٠١٣٩	0.0026
BEER-ALIS	723.993.687	723.993.722	٠,٠٠٣٥-	723.993.698	723.993.769	٠,٠٠٧١-	0.0036

Table (4): **Compared between the network base lines are computed ,when link the network by point inside the network(RARO) and when link by point outside the network (RAMO)**

Estimation of the deformation parameters

In numerous applications of deformation analyses in crustal movement studies, the final aim is a representation of the deformation in terms of strain parameters. The basic principles of strain analysis, as developed in the theory of elasticity, are applicable if the area covered by the monitoring network can be considered as a continum deforming under stress **(Abdel-Monem,1996)**. The infinitesimal homogenous horizontal strain model is used here. Vertical strain is not included in this work to avoid the less accuracy in the vertical component (**Kakkuri and Chen, 1990)**

The deformations are generally small in comparison with size of the network. So, they may be modeled by a differential relationship. Let us denote the strain rate for a line at a point P in direction $\propto_i$ with value ε_i **(Jaeger, 1964; Schneider, 1982)** then we have:

$$\varepsilon_i = \frac{\Delta s_i}{\Delta t_i \cdot s_i} = e_{xx}\cos^2\alpha_i + e_{xy}\sin 2\alpha_i + e_{yy}\sin^2\alpha_i \qquad (1)$$

Where :-

s_i is the unstrained length of the line computed (ellipsoidal distance),

Δs_i is the change in s_i during the time interval Δt_i

The rate of the strain tensor components are defined as follows:-

$$e_{xx} = \frac{1}{\Delta t} \cdot \frac{\partial u}{\partial x} \tag{2}$$

$$e_{yy} = \frac{1}{\Delta t} \cdot \frac{\partial v}{\partial y} \tag{3}$$

$$e_{xy} = \frac{1}{2\Delta t} \cdot \left(\frac{\partial u}{\partial y} + \frac{\partial v}{\partial y} \right) \tag{4}$$

Where: (u , v) being the displacement at the point P during the time interval Δt in the direction of x, y respectively.

To evaluate the strain tensor components, the strain rates must be known for at least three lines in different directions. As there are random errors in the observations, the least squares adjustment is the optimal solutions, when the number of observations in different directions from point P is greater than three in the case of observations:

$$V = Be - \varepsilon \tag{5}$$

With

$$\varepsilon^T = (\varepsilon_1 \varepsilon_2 \varepsilon_3 ..... \varepsilon_4)$$

$$B = \begin{bmatrix} \cos^2\theta_1 & \sin 2\theta_1 & \sin^2\theta_1 \\ \cos^2\theta_2 & \sin 2\theta_2 & \sin^2\theta_2 \\ \cos^2\theta_3 & \sin 2\theta_3 & \sin^2\theta_3 \\ \cos^2\theta_n & \sin 2\theta_n & \sin^2\theta_n \end{bmatrix} \tag{6}$$

$$e = \begin{bmatrix} e_{xx} \\ e_{xy} \\ e_{yy} \end{bmatrix} \tag{7}$$

where:-

V : is the residual of the observed values,

B : is the coefficient matrix, and

ε : is the observed values

To make εV^2= min., A least squares method will be done. The following equation gives the best solution of the system

$$e = \left(B^T Q_{\varepsilon\varepsilon}^{-1} B\right)^{-1} \cdot B^T Q_{\varepsilon\varepsilon}^{-1} \varepsilon \quad (8)$$

where, Q is the weight matrix obtained from the variance-covariance of coordinates of both observations epochs (**Chen 1991**).

Dilation $$\Delta = e_{xx} + e_{yy} \quad (9)$$

Pure Shear $$\gamma_1 = e_{xx} - e_{yy} \quad (10)$$

Engineering Shear $$\gamma_2 = 2e_{xy} \quad (11)$$

Total shear $$\gamma = (\gamma_1^{\,2} + \gamma_2^{\,2})^{1/2} \quad (12)$$

Principal strains $$\varepsilon_1 = \frac{1}{2}(\Delta + \gamma) \quad (13)$$

$$\varepsilon_2 = \frac{1}{2}(\Delta - \gamma) \quad (14)$$

Direction of ε_1 $$\propto = \tan^{-1}\left(\frac{e_{xy}}{\varepsilon_1 - e_{yy}}\right) \quad (15)$$

The above mentioned strain parameter are expressed in deformed body center of gravity. To compute the deformation parameters the area divided in the first method into four blocks and in the second method into five blocks. The parameters of the deformation are related to the center of a single block within the network. The horizontal components of the velocity vectors are used to estimate the strain and stress field in the study area. The calculated parameters are the maximum principal strain rate (ε1), minimum principal strain rate (ε2), direction of the maximum principal strain rate (α), annual rate of maximum shear strain (γ max) and dilatation (Δ) **(Fuji, 1997)**. The program is used for computing the strain in the main blocks center of gravity and also computing the translation T_x and T_y of these main blocks (Tables 4&5). The strain analysis is calculated between the periods from the repeated survey to the other survey. In this paper had been used the final analyses between the last epoch to the first one. Values of the parameter strain are small and sometimes are not significant in the area (Tables 4 & 5).

The areal compressions strains cover the medial region toward to the south in the present period where there is the intersection of the N-S faults with the Kalabsha fault (Fig. 4a&b). Dilatational strains show patches of high and medial values of the compression strain (Fig. 4b).

In addition to this, there are low compressional in the east and the northern part of the region (Fig. 4a) and in the east part of the region (Fig. 4b). There are some areas of low compressional strains rates.

The total amount of maximum shear strain accumulation during the present interval is relatively small and lies in lowest class according to Fuji's classifications (1995) and is prevailing in the central region where there is intersection N-S fault with Kalabsha fault (Fig. 5). The network region can be divided into three areas: high shear strain area is covering part of Khou El-Ramla fault (Fig. 5a), Kalabsha and Seiyal faults (Fig. 5b). Medial shear strain area is covering some parts; Moreover, the low shear strain rate is covering most parts of the region.

To, compare the maximum horizontal strains with the seismic data; the epicentral distributions are plotted in the figure (6). Generally, high rates of the compressional, shear strains and horizontal strains with earthquake activity in the present interval in the central part indicate that, the area is characterized by it has a property of plasticity. So, when it happens any deformation, it could be the capability to return back again to the normal case.

The present analysis shows that, the medial part of the region in the present period is dominated by compressional strain, shear strains and horizontal strains rates. This might be due to the restraining and releasing of stress in this area. From this analysis the hazards could be evaluated in Kalabsha, Seiyal and Khor el-Ramla regions. The crustal deformation processes could occur during the accumulation of the energy within the Earth’s crust and during the different paths of energy releasing. This means that the network area has been suffered from pre-, co- and post-seismic deformation during present interval period. However, a dramatic increase in general earthquake activity in this area could be to expect. The seismic activity reflects the release of energy accumulated as a result of the pressure accumulated in the area.

Magnitudes and orientation of principal axes of the strain rates across the four and five blocks of the network in the two cases are calculated and plotted in figure (7). The network area is divided to three parts. The extension is prevailing at block IV (Fig. 7a) and its orientation NE-SW direction. The compression is prevailing at block III (Fig. 7a&b) and its orientation NW-SE direction. There are some balance between compression and extension in other blocks. The results of these analyses represent the framework of the dynamic model for the deformation, which occurred in the area under investigation.

According to the stress and strain field estimations of the different epochs, the area under investigation suffers from compression and tension (stress and strain). The first principal strains

of all epochs are extension in SW-NE direction and the second principal strains are compression in SE to NW direction. The direction of a stress force is from SE to NW. The same conclusion was obtained from the focal mechanism solution of the earthquakes located in the Aswan region. This force may be due to two reasons (Schandelmeier et al., 1987; Abdel-Monem, 1996):

1. The first possible explanation (regional), results from the fact that the direction of this force is in accordance with the maximum horizontal compression induced by the approximately SE to NW drift of the African plate.
2. The second explanation (local) the force which affects to the Kalabsha and Seiyal area may be due to the effect of water loading in the lake where the direction of this force is perpendicular to the main axis of the lake.

Table (4): Station displacements and strain parameters of geodetic network from 2006 to 2010 when using RARO

Block No.	Name	Stations displacement and RMS in [m]						Principle strain rate in micro – strain	
		dx	**RMS (dx)**	**dy**	**RMS (dy)**	**dz**	**RMS (dz)**		
I	GA	0.0008	0.0018	0.0045	0.0014	-0.0162	0.0013	ε_1	5.8225E-009
	AL	0.0042	0.0018	0.0048	0.0016	-0.0041	0.0013	ε_2	-8.1325E-009
	BE	0.0023	0.0018	0.0011	0.0015	-0.0055	0.0013	α	43.9019
	AS	0.0133	0.0018	0.0109	0.0014	-0.0224	0.0013	Δ	-2.3105E-009
								λ	1.3955E-008
II	AS	0.0133	0.0018	0.0109	0.0014	-0.0224	0.0013	ε_1	1.5455E-009
	BE	0.0023	0.0018	0.0011	0.0015	-0.0055	0.0013	ε_2	-4.325E-008
	DA	0.0019	0.0018	0.0024	0.0015	-0.0002	0.0013	α	105.2770
	KL	-0.0032	0.0018	0.0111	0.0014	-0.0087	0.0013	Δ	-4.1725E-008
								λ	4.48E-008
III	KL	-0.0032	0.0018	0.0111	0.0014	-0.0087	0.0013	ε_1	7.215E-008
	DA	0.0019	0.0018	0.0024	0.0015	-0.0002	0.0013	ε_2	-1.46725E-007
	MA	0.0065	0.0019	0.0184	0.0015	-0.0083	0.0013	α	107.4994
	NM	-0.0015	0.0018	0.0183	0.0014	-0.0104	0.0013	Δ	-7.4575E-008
								λ	2.18875E-007
IV	NM	-0.0015	0.0018	0.0183	0.0014	-0.0104	0.0013	ε_1	9.44E-008
	MA	0.0065	0.0019	0.0184	0.0015	-0.0083	0.0013	ε_2	4.84E-009
	UN	0.0005	0.0021	0.0090	0.0016	-0.0124	0.0015	α	-51.3941
	RS	0.0069	0.0018	0.0136	0.0014	-0.0150	0.0013	Δ	9.925E-008
								λ	8.9575E-008

Table (6): Station displacement and strain parameters geodetic network from 2006 to 2010 (using Drag).

Block No.	Name	Stations displacement and RMS in [m]						Principle strain rate in micro – strain	
		dx	**RMS (dx)**	**dy**	**RMS (dy)**	**dz**	**RMS (dz)**		
I	GA	-0.0363	0.0025	-0.0231	0.0019	-0.0259	0.0019	ε_1	5.0725E-008
	AL	-0.0400	0.0024	-0.0271	0.0019	-0.0166	0.0019	ε_2	-3.62E-008
	BE	-0.0328	0.0024	-0.0296	0.0019	-0.0147	0.0019	α	-68.9065
	AS	-0.0280	0.0024	-0.0203	0.0018	-0.0346	0.0019	Δ	1.4545E-008
								λ	8.6925E-008
II	As	-0.0280	0.0024	-0.0203	0.0018	-0.0346	0.0019	ε_1	-9.0075E-009
	BE	-0.0328	0.0024	-0.0296	0.0019	-0.0147	0.0019	ε_2	-6.8725E-008
	DA	-0.0385	0.0024	-0.0293	0.0019	-0.0154	0.0019	α	-69.6380
	RA	-0.0251	0.0024	-0.0178	0.0018	-0.0044	0.0019	Δ	-7.7725E-008
								λ	5.97E-008
III	AS	-0.0280	0.0024	-0.0203	0.0018	-0.0346	0.0019	ε_1	5.6525E-008
	RA	-0.0251	0.0024	-0.0178	0.0018	-0.0044	0.0019	ε_2	-1.7255E-007
	NM	-0.0366	0.0024	-0.0085	0.0018	-0.0200	0.0019	α	120.0745
	KL	-0.0360	0.0025	-0.0136	0.0019	-0.0153	0.0019	Δ	-1.16025E-007
								λ	2.29075E-007
IV	RA	-0.0251	0.0024	-0.0178	0.0018	-0.0044	0.0019	ε_1	1.3125E-008
	DA	-0.0385	0.0024	-0.0293	0.0019	-0.0154	0.0019	ε_2	-1.07675E-007
	MA	-0.0253	0.0034	-0.0053	0.0026	-0.0169	0.0024	α	99.0103
	UN	-0.0331	0.0036	-0.0141	0.0028	-0.0216	0.0026	Δ	-9.455E-008
								λ	1.208E-007
V	RA	-0.0251	0.0024	-0.0178	0.0018	-0.0044	0.0019	ε_1	1.832E-008
	UN	-0.0331	0.0036	-0.0141	0.0028	-0.0216	0.0026	ε_2	-8.305E-008
	RS	-0.0251	0.0025	-0.0109	0.0019	-0.0238	0.0019	α	-89.3111
	NM	-0.0366	0.0024	-0.0085	0.0018	-0.0200	0.0019	Δ	-6.475E-008
								λ	1.01375E-007

Table (6): Classification of frequency distribution of maximum shear strain according to Fuji, (1995).

No.	Classification	Maximum shear strain		
		From	To	
1	Highest class	0.45×10^{-6}	0.36×10^{-6}	Microstrain/yr
2	High class	0.35×10^{-6}	0.26×10^{-6}	Microstrain/yr
3	Middle class	0.15×10^{-6}	0.16×10^{-6}	Microstrain/yr
4	Low class	0.15×10^{-6}	0.6×10^{-7}	Microstrain/yr
5	Lowest class	0.5×10^{-7}	0.1×10^{-7}	Microstrain/yr

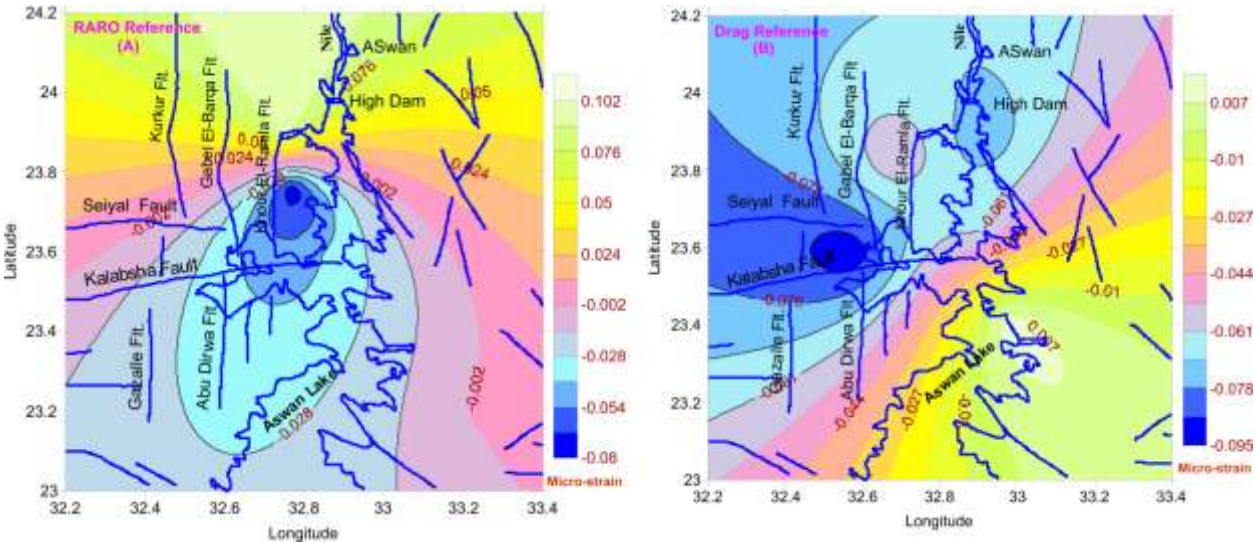

Figure (4): Distribution of the dilatation strain rates for the period from 2006 to 2010

.

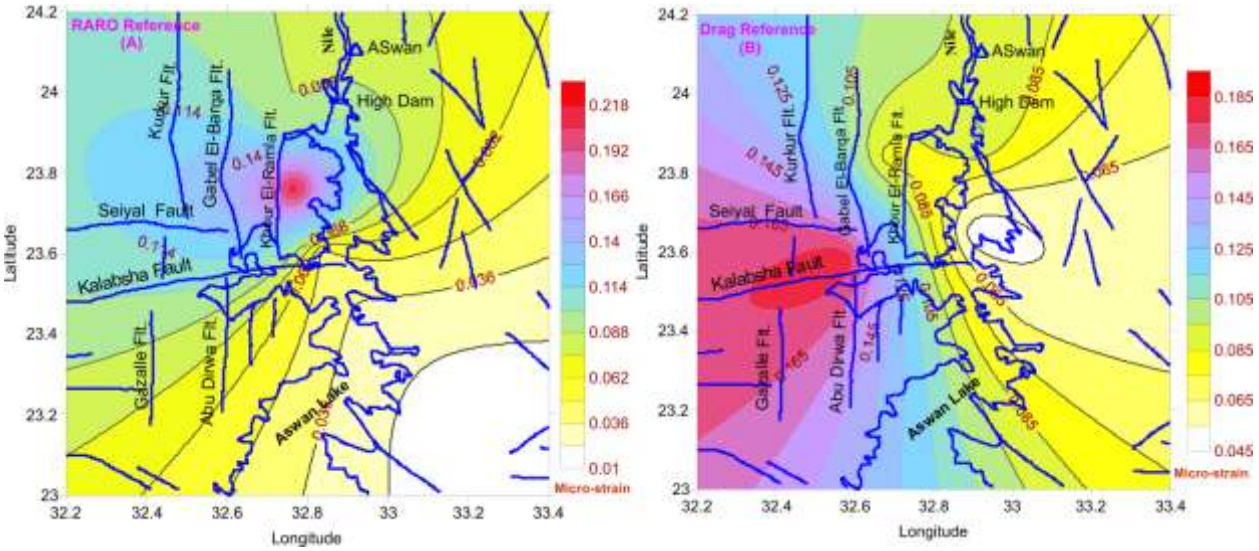

Figure (5): Distribution of the maximum shear strain rates for the period from 2006 to 2010.

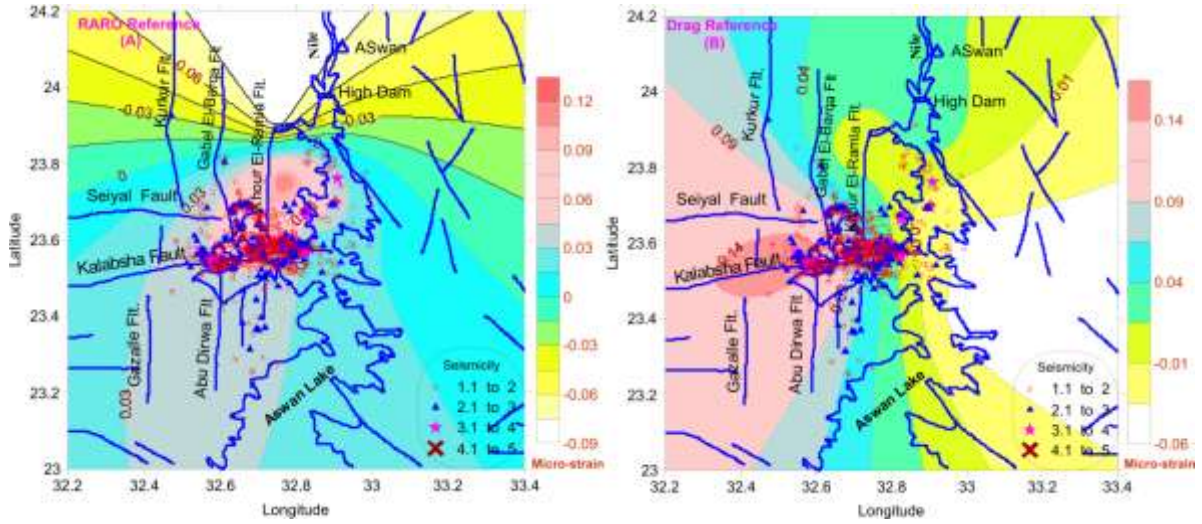

Figure (6): Distribution of the total horizontal strain rates and the seismicity for the period from 2006 to 2010.

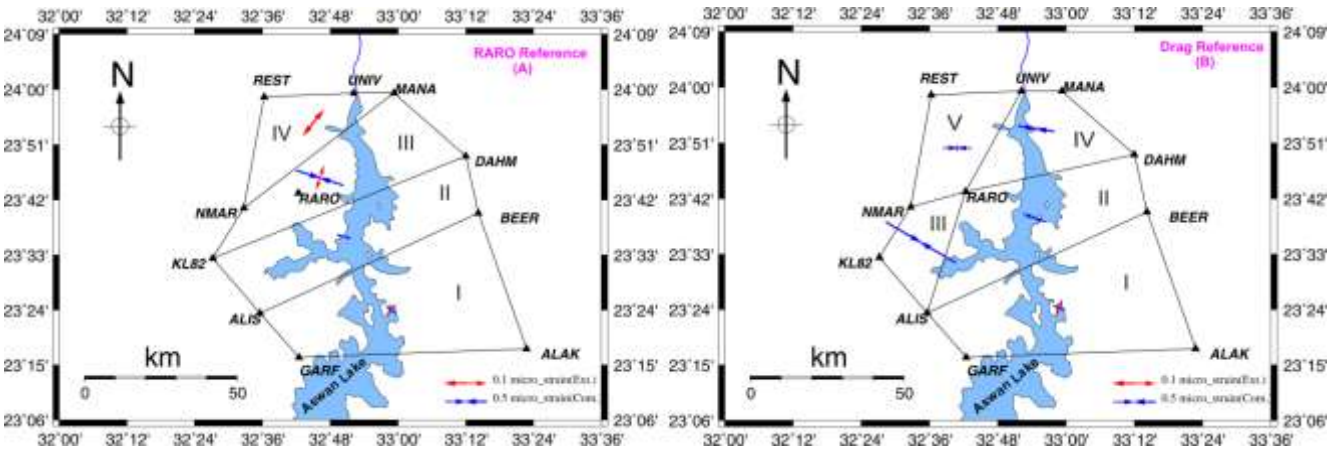

Figure (7): Magnitude and orientation of principal axes of the strain rates for the period from 2006 to 2010.

Discussion and conclusion

The crustal deformation in the seismically active areas in Aswan were examined, as obtained from both seismological and GPS data. The results from data sets are compared and combined in order to determine the main characteristics of deformation and hazard estimation for the specified areas in Aswan. Comparing the geodetic results with the seismic activity in the area, a relationship between the accumulated energy releases associated with the earthquake occurrences and the deformation found. The seismic activity reflects the release of energy accumulated as a result of the pressure accumulated in the area. The strain rate tensors estimated in this study show compression and extension components directed in NW-SE and NN-SW that consistent with the T-axes and P-axes derived from earthquake fault plane solutions, respectively. The simple blocks model suggests that Aswan region is characterized by Compressional and extensional deformation that consistent with earthquake focal mechanisms and in agreement with the previous kinematics models of this area.

The aim of this study is to determine the accuracy of test results when they are linked to the network with stations from outside or from within. The final compiled output from the seismic and geodetic analysis will focus on the geodynamical regime of the seismo-active region and it is an attempt to delineate the crustal stress and strain fields. The conclusions of this study

try to present a clear preliminary picture of crustal deformation at Aswan region and their role in earthquake occurrence and prediction. On the basis of this dataset the following concluding remarks can be drawn:

1- Linking the network with outside station gives more accurate results than if it is linked with inside station.
2- Bernese software program gives more accurate results with long base lines than short base lines.
3- The strain accumulations and the earthquake activity are concentrated on the intersection area between Kalabsha fault with N-S faults.
4- The area is characterized by it has a property of plasticity. So, when it happens any deformation, it could be the capability to return back again to the normal case.
5- According to the stress and strain field estimations of the different epochs, Aswan region has suffered from tension and compression.
6- The prevailing direction of the extension is in SW-NE and the compression is in SE- NW direction.
7- The direction of the compression force is from SE to NW. The same conclusion was obtained from the focal mechanism solution of the earthquakes located in the Aswan region. This force may be due to two reasons: a- Locally, (Kalabsha and Seiyal area) effect of the water loading in the, where the direction of this force is perpendicular to the main axis of the lake. b- Regionally, (whole Aswan region) the direction of this force is in accordance with the maximum horizontal compression induced by the approximately SE to NW drift of the African plate.

Acknowledgements

The authors are very grateful to the staff members of the Crustal Movement Laboratory of the National Research Institute of Astronomy and Geophysics for their participation in GPS data collection.

References

Abdel-Monem S. M., (1996): Geodynamics and Seismicity of the Seiyal Area, Northwestern Part of Aswan Lake, Egypt. Candidates Ph.D. Dissertation. Geodetic and Geophysical Research Institute, Sopron, Hungary.

Abdel-Monem S. M., (2001): The Study of Recent Vertical Crustal Movements in Aswan Region, Egypt. NRIAG Bulletin, Geophysics (B) pp. 25-41.

Abdel-Monem S. M., (2005): Using compiled seismic and GPS data for hazard estimation in Egypt. NRIAG, Journal of Geophysics,Vol.4, No. 1, pp. 51-79.

Abdel-Monem S. M., (2010): Water-level variation in the reservoir and triggered seismicity in Aswan region. (Under publishing)

Caspary W. F. (1987): Concepts of Network and Deformation Analysis. School of Surveying, the University of New South Wales, Australia,183 pp.

Chen R. (1991): Horizontal Crustal Deformations in Finland . Reports of the Finish Geodetic Institute , 91:1.

Dach, (2007):- Processing Example Introductory Course Terminal Session .Astronomical Institute, University of Bern.

Fuji, Y., (1995): Characteristics Of Horizontal Crustal Deformation In Japan As Deduced From Frequency Distribution Of Maximum Shear Strain Rate, Pageoph, Vol. 144, No. 1 (1995), Birkhauser Verlag, Basel. pp. 19-37.

Fuji Y., (1997): Estimation of continuous distribution of Earth's strain in the Kanto-Tokai district, Central Japan, with the aid of least squares collocation. An advanced lectures on geodesy and seismology in Egypt August, 1996-July, 1997. Bulletin of NRIAG (Special Issue). pp. 97- 126.

Issawi B., (1969): The Geology of Kurkur-Dungul Area. General Egyptian Organization for Geological Research and Mining; Geological Survey. No. 46, 101 pp. Cairo, Egypt.

Issawi B., (1978): Geology of Nubia West Area, Western Desert. Annals of the Geological Survey of Egypt. vol. B, pp.237-253.

Jaeger J.C. ,(1964):- Elasticity , Fracture and F low , with Engineering and Geological Applications , Methuen, London.

Kakkuri J. and Chen R. (1991):- Finnish Geodetic Institute Ilmalankatu IA, SF- 00246 Helsinki ,Finland.

Rothe, J. R. (1968): Fill a lake, start an earthquake. New Scientist, Vol. 39, pp. 75-78.

Sohrab, S. (1972): Earthquakes related to reservoir filling, National Academy of Sciences, Washington.

Vyskočil, P.; Kebeasy, R.M.; Tealeb, A.; and Mahmoud, S.M., (1989): The present state of recent crustal movement studies at Kalabsha area, Aswan, Egypt. Proc. 6th Intern Symp. "Geodesy and Physics of the Earth", Potsdam, PP. 301-333.